Journal Pre-proof

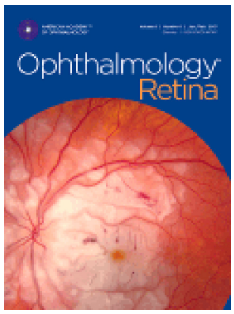

CERKL-associated retinal dystrophy: Genetics, Phenotype and Natural History

Malena Daich Varela, MD, Emma S. Duignan, Samantha R. De Silva, DPhil, FRCOphth, Rola Ba-Abbad, PhD, FRCS (Glasg), Yu Fujinami-Yokokawa, MPH, Shaun Leo, MSc, Kaoru Fujinami, MD, PhD, Omar A. Mahroo, PhD, FRCOphth, Anthony G. Robson, PhD, Andrew R. Webster, MD(Res), FRCOphth, Michel Michaelides, MD(Res), FRCOphth

PII: S2468-6530(23)00258-0

DOI: https://doi.org/10.1016/j.oret.2023.06.007

Reference: ORET 1468

To appear in: *Ophthalmology Retina*

Received Date: 23 February 2023

Revised Date: 9 June 2023

Accepted Date: 12 June 2023

Please cite this article as: Daich Varela M., Duignan E.S., De Silva S.R, Ba-Abbad R., Fujinami-Yokokawa Y., Leo S., Fujinami K., Mahroo O.A, Robson A.G., Webster A.R. & Michaelides M., *CERKL*-associated retinal dystrophy: Genetics, Phenotype and Natural History, *Ophthalmology Retina* (2023), doi: https://doi.org/10.1016/j.oret.2023.06.007.

CERKL-associated retinal dystrophy: Genetics, Phenotype and Natural History

Running head: *CERKL*-associated retinal dystrophy

Malena Daich Varela, MD[1, 2]	m.daichvarela@ucl.ac.uk
Emma S. Duignan[3]	emmaduignan@rcsi.ie
Samantha R De Silva DPhil, FRCOphth[1,2]	samantha.desilva@nhs.net
Rola Ba-Abbad, PhD, FRCS (Glasg)[4]	rola.baabbad.09@alumni.ucl.ac.uk
Yu Fujinami-Yokokawa, MPH[2, 5, 6]	y.fujinami@keio.jp
Shaun Leo, MSc[1]	shaun.leo@nhs.net
Kaoru Fujinami, MD, PhD[1, 2, 5]	k.fujinami@ucl.ac.uk
Omar A Mahroo, PhD, FRCOphth[1, 2]	o.mahroo@ucl.ac.uk
Anthony G. Robson, PhD[1, 2]	anthony.robson3@nhs.net
Andrew R. Webster, MD(Res), FRCOphth[1, 2]	andrew.webster@ucl.ac.uk
Michel Michaelides, MD(Res), FRCOphth[1, 2] *	michel.michaelides@ucl.ac.uk

[1] Moorfields Eye Hospital, London, United Kingdom.

[2] UCL Institute of Ophthalmology, University College London, London, United Kingdom.

[3]Royal Victoria Eye and Ear Hospital, Dublin, Ireland.

[4]Ocular Genetics Services, King Khaled Eye Specialist Hospital, Riyadh, Saudi Arabia

[5] Laboratory of Visual Physiology, Division of Vision Research, National Institute of Sensory Organs, National Hospital Organization Tokyo Medical Center, Tokyo, Japan.

[6] Department of Health Policy and Management, School of Medicine, Keio University, Tokyo, Japan.

*Corresponding Author:

Professor Michel Michaelides

UCL Institute of Ophthalmology

11-43 Bath Street, London, EC1V 9EL, UK

michel.michaelides@ucl.ac.uk

Meeting presentations: This work has not been presented in any meeting or conference.

Financial support: This work was supported by grants from The Wellcome Trust [099173/Z/12/Z], the National Institute for Health Research Biomedical Research Centre at Moorfields Eye Hospital NHS Foundation Trust and UCL Institute of Ophthalmology, Moorfields Eye Charity, Retina UK and the Foundation Fighting Blindness (no specific grant/award number for the latter). The views expressed are those of the authors and not necessarily those of the NHS, the NIHR or the Department of Health.

Conflict of interest: The authors alone are responsible for the content and writing of this article. MM consults for MeiraGTx Ltd.

Abstract

Purpose: To analyze the clinical characteristics, natural history, and genetics of *CERKL*-associated retinal dystrophy in the largest series to date.

Design: Multicenter retrospective cohort study.

Subjects: 47 patients (37 families) with likely disease-causing *CERKL* variants

Methods: Review of clinical notes, ophthalmic images, and molecular diagnosis from two international centres.

Main outcome measures: Visual function, retinal imaging and characteristics were evaluated and correlated.

Results: The mean age at the first visit was 29.6 ± 13.9 years and the mean follow-up time was 9.1 ± 7.4 years. The most frequent initial symptom was central vision loss (40%) and the most common retinal feature was well-demarcated areas of macular atrophy (57%). Seventy percent of the participants had double-null genotypes and 64% had electrophysiological assessment. Amongst the latter, 53% showed similar severity of rod and cone dysfunction, 27% revealed a rod-cone, 10% a cone-rod, and 10% a macular dystrophy dysfunction pattern. Patients without double-null genotypes tended to have fewer pigment deposits and included a higher proportion of older patients with a relatively mild electrophysiological phenotype.

Longitudinal analysis showed that over half of the cohort lost 15 ETDRS letters or more in at least one eye during the first 5 years of follow up.

Conclusions: The phenotype of *CERKL*-retinal dystrophy is broad, encompassing isolated macular disease to severe retina-wide involvement, with a range of functional phenotypes, generally not fitting in the rod-cone/cone-rod dichotomy. Disease onset is often earlier, with more severe retinal degenerative changes and photoreceptor dysfunction, in nullizygous cases.

Introduction

Inherited retinal diseases (IRDs) are a group of heterogeneous stationary or progressive retinal disorders, that often cause visual impairment.[1] IRDs represent a leading cause of visual disability in the working age population in the UK.[2] Depending on whether rod or cone photoreceptors are primarily (or more severely) affected, two main phenotypes of IRD can be differentiated – cone-rod (CORD) and rod-cone dystrophy (RCD); the latter also known as retinitis pigmentosa (RP). Macular dystrophy (MD) corresponds to an IRD where dysfunction is confined to the macula. Halting the progression of these conditions and alleviating their symptoms is the subject of multiple avenues of research.

Over 300 genes and loci are currently known to cause IRD (https://web.sph.uth.edu/RetNet/). Ceramide-kinase like (*CERKL*, MIM 608381) is amongst the rare causative genes in the UK, detected only in 17 families of a large cohort of over 3000 genetically diagnosed IRD families by 2020.[3] It is also reported to be an uncommon cause of CORD in a German cohort.[4] Other groups however, report a higher prevalence of *CERKL*-associated retinopathy, accounting for 33% and 5% of autosomal recessive IRD in Yemenite Jewish and Spanish populations, respectively.[5,6] *CERKL* was associated with 8% of IRD cases in Tunisia,[7] and was one of the commonest genes in a large Spanish RP cohort study.[8] To date, four founder disease-causing variants have been described; NM_001030311.2: c.847C>T (p.Arg283Ter) (reported as NM_201548.5: c.769C>T) from Spain, c.238+1G>A from the Yemenite Jewish population, c.375C>G (p.Cys125Trp) from the Finnish, and c.365T>G (p.Leu122Arg) from indigenous African populations in South Africa.[5,9–11]

CERKL was first associated with IRD in 2004, after Tuson *et al.* analyzed RP26, a 17.4 Mb locus in chromosome 2 known to cause RP in Spanish families.[9] It is a 13-exon gene that encodes a 532-amino acid protein, with a diacylglycerol kinase and a pleckstrin homology domains.[12] It is widely expressed in the kidney, lung, skin, and pancreas; and it is known to have a protective role against oxidative stress-induced apoptosis.[13] It also interferes with mitochondrial metabolism, stress granules, and autophagy regulation; yet its pathophysiology remains to be fully elucidated.[14]

Biallelic loss-of-function variants in *CERKL* have been associated with both RCD and CORD.[15,16] However, the reported retinal phenotype in both cases appears to be somewhat

similar: a widespread retinopathy with early maculopathy and a similar severity of rod and cone dysfunction electrophysiologically.[5,15] Patients often report concurrent cone- (e.g., central vision and colour discrimination impairment) and rod-related (e.g., nyctalopia, peripheral field loss) symptoms, becoming noticeable from adolescence/young adulthood, with an unclear timeline.[17] *CERKL* can also present with a Stargardt-like phenotype, often being a differential diagnosis when no variants are found in *ABCA4*. Nevertheless, there remains a paucity of detailed phenotypic characterization in a large cohort, thereby limiting our understanding of *CERKL*-associated retinopathy and its natural history. This study aims to establish the phenotypic and genetic spectrum by examining the largest case series of *CERKL*-associated retinopathy patients to date, to better understand this disorder and to optimize future clinical management.

Methods

This study was a retrospective, consecutive case series of patients who attended Moorfields Eye hospital (MEH, London, UK) and the Royal Victoria Eye and Ear Hospital (Dublin, Ireland) with a retinal dystrophy, and were found to have likely disease-causing variants in *CERKL*. At MEH, patients were identified through the inherited eye disease database. Informed consent was obtained from all patients. Ethical approval was provided by the local ethics committee and the study honored the tenets of the Declaration of Helsinki.

Relevant patient data was retrieved from electronic healthcare records, case notes, and imaging software systems. Snellen visual acuities were recorded and converted to LogMAR for the purpose of statistical analysis. Count fingers vision was given a value of LogMAR 1.98, hand motion LogMAR 2.28, light perception LogMAR 2.7, and no light perception LogMAR 3.[18] Asymmetric best-corrected visual acuity (BCVA) was defined as a difference ≥0.3 LogMAR (equivalent to 15 Early Treatment Diabetic Retinopathy Study -ETDRS- letters) between eyes. Patients were categorized using the World Health Organization (WHO) visual impairment criteria, that defines no or mild visual impairment as BCVA $\leq$ 0.48 (6/18, 20/60), moderate impairment as BCVA > 0.48 and $\leq$ 1.0 (6/60, 20/200), severe as BCVA >1.0 and $\leq$ 1.3 (3/60, 20/400), and blindness as BCVA > 1.3. Records of visual field were limited within our cohort; therefore, we classified patients according to BCVA only. 'Low vision' corresponds to patients with moderate and severe visual impairment.

Further clinical assessment consisted of dilated fundus examination, spectral-domain optical coherence tomography (SD-OCT, Heidelberg Spectralis, Heidelberg Engineering, Inc., Heidelberg, Germany), fundus autofluorescence (Heidelberg Spectralis, Heidelberg Engineering, Inc., Heidelberg, Germany and Optos PLC, Dunfermline, UK) and ultrawide field fundus pseudocolor photography (Optos PLC). OCT thickness in the general population was extracted from Invernizzi *et al*.[19] Fovea-centered macular volume scans were performed in a 6-mm^2 area that included the 1-, 3-, and 6-mm grid templates from the ETDRS. Inner limiting membrane and Bruch membrane were automatically segmented by the manufacturer software (Heyex version 1.9.14.0; Heidelberg Engineering) and adjusted manually as needed by a trained ophthalmologist (M.D.V.). Ellipsoid zone (EZ) width and outer nuclear layer thickness (ONLT) were measured manually at the foveal scan. Patients with macular cysts, oedema, and/or only line scans were excluded from quantitative assessment. Non-ocular issues were defined as those commonly found in syndromic IRDs, such as musculoskeletal, renal, cardiac, audiologic, or neuro/psychological.[20]

Pattern and full-field electroretinogram (PERG; ERG) testing was performed incorporating the International Society for Clinical Electrophysiology of Vision (ISCEV) standards.[21] Pattern ERG P50 was used as an objective measure of macular function and full-field ERG was used to assess generalized (mainly peripheral) rod and cone system function. The main dark-adapted (DA) and light-adapted (LA) ERG components were quantified and compared with age-matched control data from healthy subjects (age range: 10-79 years).[22] ERG amplitudes were plotted as a percentage of the age-matched lower limit of the reference range or as a difference from the age-matched upper limit of peak time. The reference limits were defined as lower 5th percentile for amplitude and 95th percentile for peak times. The full-field ERGs were classified into 4 groups based on the relative reduction of DA and LA ERGs; rod and cone photoreceptor dysfunction, rod-cone, cone-rod or predominantly macular dysfunction (normal or near-normal ERGs). For the purposes of the electrophysiological analysis, a 33% minimum difference in the relative reduction of DA 10 ERG a-wave and LA 3 ERG b-wave was used to define rod-cone and cone-rod patterns of dysfunction. An additional patient (age 5 years, ID 41) was tested before his baseline ophthalmologic assessment according to shorter PERG and ERG protocols using lower eyelid skin electrodes without mydriasis.

DNA was extracted from whole blood and genetic testing was performed using panel-based targeted next generation sequencing (NGS), whole exome sequencing, or whole genome sequencing. Where appropriate, blood samples were taken from parents or siblings to confirm segregation of proposed variants (i.e., to determine if relatives carry one or both variants in one or two alleles). Other IRD genes were excluded based on coding variant analysis. The pathogenicity of the variants was determined by implementing the criteria of the American College of Medical Genetics (ACMG).[23] Likely disease-causing variants correspond to pathogenic, likely pathogenic, and selected variants of uncertain significance (VUS), based on family history, phenotype, and/or if concurrent with a pathogenic/likely pathogenic variant. *In silico* molecular genetic analysis was performed for all detected *CERKL* variants (Genome reference; Hg38 Transcript; NM_001030311.2, ENST00000339098.9 or NM_201548.5, ENST00000410087.8), according to a previous publication.[24] Genotype grouping was performed according to the presence of null variants (those assumed to result in a loss of function - nonsense, frameshift, splice site alteration, and exon deletion-); a double-null (DN) genotype harboring multiple null variants (also known as 'nullizygous'), and a non-double-null (NDN) genotype with one or no null variants. Clinical descriptions and parameters were compared between subgroups of patients with DN and NDN genotypes.

GraphPad Prism 8.0.2 (GraphPad Software, San Diego, CA, USA) was used for statistical analysis. The threshold of significance was set at $p < 0.05$. Linear regressions and t-tests were used for assessment of parametric variables. When testing associations between age and ocular characteristics, only the right eye was considered to avoid clustering effect. Welch's t-test variation was employed when the sample sizes were significantly different.

Results

Demographics, phenotype, and visual acuity

Forty-seven patients were characterized from 37 pedigrees. Their clinical characteristics are listed in Table 1 and Supplementary Table 2. Twenty-two individuals were female (47%) and 25 (53%) were male. The mean age ± standard deviation (SD) at the first visit was 29.6 ± 13.9 years (range ~~8~~ 6 – 67 years) and the median age was 25 years, with 5 participants (11%) having their

first visit below the age of 16. The mean follow-up time of the cohort was 9.1 ± 7.4 years and the mean age at their final visit was 39.2 ± 16.6 years. One patient was deaf and had an autosomal dominant family history of deafness; no other participant had non-ocular ~~features~~ issues. Amongst the patients that reported their ethnicity (72%), 19 were of Asian origin, 13 were white from UK and Europe, and 2 were of African descent. Consanguinity was reported in six families, where parents were first cousins.

Based on ophthalmic history and clinical examination, 26 patients were initially diagnosed with RP (RCD), 13 with CORD, and 8 with macular dystrophy (MD). The mean age of symptoms onset was 19.8 ± 9 years (median 17, range 6-47 years), with 16 patients below the age of 16. Nineteen patients (40%) described central vision loss as their initial symptom, 16 (34%) reported concurrent blurred central vision and nyctalopia, 5 (11%) reported night blindness first, and the remaining patients mentioned being initially bothered by scotomas, photophobia, or poor color discrimination. A prolonged prodromal history of subtle VA decrease was elicited in six patients (24%), lasting between 1 and 10 years.

Mean baseline BCVA was 0.7 ± 0.8 LogMAR OD (median 0.3) and 0.8 ± 0.8 OS (median 0.4). In those aged 15-24 years (23 participants), BCVA ranged from 0.0 LogMAR to light perception (LP, mean 0.5 ± 0.6 LogMAR, median 0.3, Figure 1A & B), 18 had none or mild visual impairment, and 5 had moderate visual impairment. There were 13 patients aged 25-40 years old whose BCVA ranged from 0.0 LogMAR to hand movements (mean 0.7 ± 0.7, median 0.4), 8 had no or mild visual impairment, 3 had moderate visual impairment, 1 had severe, and 1 was blind. Amongst those over 40 years old (11 individuals), BCVA was between 0.2 LogMAR and LP (mean 1.4 ± 1.1, median 0.8), 6 had no or mild impairment, and 5 were blind. Asymmetric BCVA was seen in 10 patients (21%; 4 in the 15-24 years old group, 5 in the 25-40 years old group, and 1 in the 41 and older subgroup). Analyzed cross-sectionally, there was a significant association between age and BCVA for both OD ($p = 0.0002$) and OS ($p < 0.0001$, Figure 1C).

Refractive data was available for 23 patients (49%), with a mean spherical equivalent of -1.9 ± 2.8 diopters (D). Of these, seventeen patients (74%) had a mild myopic and hyperopic spherical equivalent (-3 to +3 D), and the remaining 6 had moderate and high myopia.

Clinical examination, color fundus photography and fundus autofluorescence imaging

Corneal examination was unremarkable in all cases. Eleven individuals (23%) developed lens opacities, at a mean age of 46.3 ± 15.2 (range 26 – 73). There was no evidence of high intraocular pressure or glaucoma in any patient.

Ultrawide-field (UWF) pseudocolor fundus and autofluorescence (AF) imaging was available in 39 participants (82%). The most common retinal feature was the presence of well-demarcated areas of atrophy at the macula, present in 27 patients (57%), from as early as 16 years of age. Fine hyperautofluorescent dots at the macula and perimacula (not visible on examination or colour), were also seen in 23 patients (49%, 6 to 60 years of age), and peripheral punched-out areas of chorioretinal atrophy were present in 21 patients (45%, Table 1) from 23 years of age, resembling a more extensive choroideremia-like pattern in patients with advanced disease.

Eighteen patients did not have pigment deposits (38%, ages 6 to 64), 15 had minimal bone-spicule-like (BSL) or nummular pigment (32%, 23 to 72 years old), 3 had moderate BSL deposits (6%, 32 to 42 years old), and 6 had dense, diffuse BSL pigment (13%, 34 to 79 years of age). By assessing their imaging, 11 patients (23%) had predominantly macular involvement, 11 (23%) had a prevailing peripheral involvement, and 17 (36%) had widespread retinal dystrophy affecting the posterior pole and the peripheral retina similarly (Figure 2 and Supplementary Table 2).

Common IRD signs were also present in this cohort, such as peripapillary atrophy (seen in 35 patients, 74%) and a hyperautofluorescent ring at the posterior pole, appearing either entirely inside the temporal vascular arcades (11 patients) or also encompassing the optic disc (5 individuals, Figure 3A). Other less frequent features were hypoautofluorescent nummular dots that followed the vascular arcades (5 patients, Figure 3B), a mottled retinal AF pattern (3 young patients, Figure 3C), foveal-sparing maculopathy (3 patients), and abnormal AF patterns, with preserved mid-peripheral retina (4 patients, Figure 3D).

Macular OCT analysis

Forty-one individuals had macular OCT scans, Heidelberg blue autofluorescence (BAF) and infrared (IR) imaging (87%).

Baseline central macular thickness (CMT) was 180.2 ± 36.0 µm, at 30.2 ± 13.8 years old (range 7 – 71). ONLT was quantifiable in 33 patients (66 eyes, 80%, 7 – 51 years old), with a mean value of 38.7 ± 24.4 µm. Both CMT and ONLT were significantly lower compared to the unaffected population ($p < 0.0001$). Foveal EZ was present in 28 patients (52 eyes, 7 to 51 years old) with a mean width of 350.5 ± 302.9 µm. A subfoveal hyporeflective zone (HRZ) was seen in 4 eyes (3 patients, 31 to 50 years old). Considering cross-sectional data only, a significant association was observed between older age and narrower EZ width ($p = 0.05$), and no significant association was found between age, CMT and ONLT ($p = 0.08$ and 0.35). No significant association was found between BCVA and EZ, CMT and ONLT ($p = 0.22$ to 0.65).

Subretinal hyperreflective material was the most common finding, present in 36 individuals (88%, Figure 4), and this was often correlated with fine hyperautofluorescent dots detected with BAF. These dots were noticed in the posterior pole or surrounding it in 29 patients (71%) and were not discernible with IR imaging. Other findings were hyperreflective material in the inner retina (33 individuals, 80%), epiretinal membrane (ERM, in 27 patients, 66%), and cystoid macular oedema, present in 3 patients (2 with RP and 1 with CORD).

Electrophysiological assessment

Thirty patients had electrophysiological assessment (64%, Tables 1 and 2). Sixteen of them showed a similar degree of DA and LA ERG reduction, in keeping with a moderate to severe rod and cone photoreceptor dystrophy, including seven (ages 15-30 years) with undetectable DA and LA ERGs. The ERG findings in others revealed a rod-cone (N=8; age range 14-51 years; median 24 years) or cone-rod (N=3; age range 15-28 years) pattern of dysfunction, with a further three showing normal or near-normal ERG amplitudes (cases 28-30; Figure 5; ages 26, 45 and 47 years). The LA 30Hz ERG peak times were normal or borderline (equal to 95th percentile) in the 3 cases with preserved ERG amplitudes (MD group). LA 30Hz ERG peak times were worse in the 13 patients with the smallest detectable ERGs (median delay 13ms) and were normal or borderline in the remaining ten, including the five oldest patients (ages 45-51 years).

Comparison of ISCEV-standard DA 0.01, DA 3 and DA 10 ERG a- and b-waves, LA 30Hz ERG and LA 3 (single flash) ERG b-waves revealed a high degree of interocular symmetry in amplitudes (slope = 1.03; r^2= 0.98) and peak times (slope = 1.02; r^2=0.99). Figure 5 summarizes the electrophysiological findings (right eyes) and patient ages at the time of testing and Figure 6 shows representative recordings.

There was no significant correlation between age and the amplitudes of the DA 0.01 ERG, DA 10 ERG a- and b-waves, LA 30Hz ERG or LA 3 ERG b-waves or the peak times of the LA 30Hz ERG. Pattern ERG P50 was undetectable in 24 patients in keeping with severe macular dysfunction. Of the remaining 6 cases, including two with MD, the PERG P50 component was reduced by 45-60% (Figure 5A). Flash ERGs in the five-year old child tested with skin electrodes showed only residual photopic ERGs, markedly subnormal scotopic bright flash ERGs and an undetectable PERG P50 component (data not shown), consistent with a photoreceptor dystrophy with severe macular involvement.

Follow-up ERG data were available in three patients (Supplementary Figure 7), showing rod-cone (ID 21) or cone-rod (IDs 19 and 20) patterns of dysfunction at baseline. In patient 21 there was marked reduction in all detectable ERG components and a 15ms increase in LA30Hz ERG peak time over a 13-year period (from age 14-27 years). In patient 19 there was rapid reduction in DA ERG amplitudes with no significant change in LA ERG amplitudes or peak times (from age 15-16 years). In patient 20 there was significant reduction in all ERG components with borderline (2ms) worsening in LA 30Hz ERG peak time (from age 18 to 23 years).

Longitudinal analysis

Mean follow up time was 9.1 $\pm$ 7.4 years (range 0-21). Follow up BCVA was available in 34 (72%) patients and was 1.5 $\pm$ 1 LogMAR OD (median 1.65) and 1.65 $\pm$ 1.05 OS (median 2.28, mean age 42 $\pm$ 14 years). The rate of BCVA decline was 0.08 LogMAR (4 letters)/year and there was a significant difference between baseline and follow up BCVA ($p < 0.0001$).

During the first five-years of follow up (n=34), the rate of BCVA decline was 0.08 LogMAR (4 letters)/year for both the overall cohort and for the group aged 15-24 years old, 0.13 (6.5 letters)/year for the 25-40 years old group, and 0.04 (2 letters)/year for the 41 and older

subgroup. During years 5-10 of follow up (n=23), the rate was 0.09 LogMAR (4.5 letters)/year for the 25-40 years old group, and 0.05 (2.5 letters)/year for the older subgroup. Lastly, during the period of 10-15 years of follow up (n=12), the group aged 25-40 years old had a decrease rate of 0.08 LogMAR (4 letters)/year, and the older subgroup of 0.06 (3 letters)/year.

Twenty-five patients out of the 34 with longitudinal data (74%) had a decrease in BCVA of 15 ETDRS letters or more over follow up in at least one eye, 20 (59%) during the first 5 years since their baseline visit. Seventeen patients (50%) progressed to more advanced WHO categories of visual impairment over follow up, 11 (32%) of whom became blind.

Thirty-three individuals had longitudinal macular OCT scans during a period of up to 12 years (mean of 6.4 $\pm$ 3.5). Longitudinal analysis demonstrated significant differences between baseline and follow up CMT ($p < 0.0001$, -5.9 µm/year), ONLT ($p < 0.0001$, -2.7 µm/year), and EZ width ($p < 0.0001$, -34.5 µm/year). Two thirds of the patients had decreased CMT over follow up and one third had increased values. The ONL was noticed to be isointense to contiguous layers, less distinct and unable to be quantified in 9 patients over the follow-up period. The association between BCVA and EZ, CMT and ONLT remained not significant ($p = 0.16$ to 0.57). Fifteen out of 16 patients with a hyperautofluorescent ring at the posterior pole had a follow up assessment. In 9 patients the ring grew in diameter, in 5 it became smaller, and in one it faded.

Molecular Genetics

All patients had biallelic/multiple rare variants in *CERKL*, and their molecular characteristics are listed in Supplemental Table 3. Thirty-two patients had homozygous variants. Twenty-three different variants were present in our cohort; 7 nonsense, 6 splice-site alteration (3 canonical splice site, 2 intronic deletions, and 1 intronic change), 6 missense, 2 small deletions/frameshift, and 2 large deletions. Eight were classified as pathogenic, 8 as likely pathogenic, and 8 as VUS. Nine (39%) were novel variants, and 14 were previously reported elsewhere. Schematic representation of these detected variants and the status of evolutionary conservation are presented (Figure 8 and Supplementary figure 9).

The most common variant was p.(Arg283Ter), encountered in 17 homozygous patients and in 6 presumed compound heterozygotes. The second most frequent variant was p.(Arg106Ser),

present in 4 homozygotes and 2 compound heterozygotes. Thirty-six participants (77%) had DN genotypes (nonsense, frameshift, splicing, or exon deletion), 4 were compound heterozygous of a null and a missense variant, and 7 had two missense changes (11 NDN, Supplementary Table 3). One patient (ID 30) was homozygous for a VUS and had a phenotype that matched *CERKL*-retinopathy, hence he was included in the cohort and considered as a likely *CERKL*-associated case.

Genotype-phenotype correlation analysis

Fifteen out of the 16 patients with childhood-onset symptoms had DN genotypes. The mean age of onset in individuals with NDN variants was 22.8 $\pm$ 9.3 years (median 18.5), and 19.5 $\pm$ 8.7 for DN (median 19, $p = 0.36$). At baseline, the 5 patients aged 15-24 years with moderate visual impairment harbored DN variants; the 5 patients aged 25-40 years with moderate visual impairment or worse were DN, and amongst those over 40 years old, 4 out of 5 blind were DN. The rate of VA decline was 0.07 $\pm$ 0.07 LogMAR/year in the NDN group and 0.08 $\pm$ 0.08 LogMAR/year in the DN group. There were no significant differences between DN and NDN groups regarding rate of progression, and no specific variant was found to be consistently milder than the others or associated with a particular phenotype.

Regarding fundus features, 8 out of 11 (73%) NDN patients had no pigment deposits, and the remaining 3 had minimal BSL pigment (age 20 to 72). In contrast, among 25% of patients with DN genotypes (n=28 with UWF imaging), 8 had no pigment deposits (29%, ages 14 to 64), 10 had minimal pigment, 3 had moderate, and 4 had dense/diffuse pigmentary changes (aged 34 to 79 years old). The presence of a ring of increased AF at the posterior pole was noted in 50% of DN patients (14/28) and 27% of NDN (3/11).

Concomitant peripheral and macular circumscribed areas of atrophy were observed in 4 patients with NDN genotypes, versus in 15 with DN genotypes. The DN subgroup included 6 patients with more marked central retinal involvement, 13 with similar central and peripheral involvement, and 9 with the peripheral retina mostly affected. The NDN group consisted of 5 patients who had a predominantly macular involvement, 4 who had similar central and peripheral involvement, and 2 who had a more peripheral degeneration (Table 2).

The ERG abnormalities were most severe (DA10 ERG a-wave reduction) in 18 of 21 with a DN genotype, including 7 with undetectable ERGs. The 9 individuals harboring NDN variants included 3 of the 5 oldest subjects tested, with 3 of the 5 mildest ERG phenotypes (2 with MD; Figure 5). Of the 10 patients with normal or borderline LA30Hz ERG peak times, 6 harbored NDN variants.

There was significant concordance of phenotype within families, with seven sets of siblings displaying similar phenotypes, including degree of pigment deposits and atrophic patches, and a similar age of onset (± 5 years). Interestingly, three young siblings were diagnosed with RP and had a comparable presentation, whereas their mother had a CORD phenotype (IDs 8, 13, 40 and 41). No correlations were found regarding variants' location or gene domain and phenotype.

Discussion

This study examines the detailed clinical and functional phenotype in the largest cohort of genetically characterized patients with *CERKL*-associated retinopathy to date. The description of the uncommon MD presentation is extended. Nine novel disease-causing variants are identified, and genotype-phenotype correlations examined. Comprehensive retinal imaging, quantitative electrophysiological and natural history data are detailed, aimed at facilitating the diagnosis and establishing rates of disease progression, to inform future patient management.

CERKL-retinopathy has been categorized to date as either presenting as RCD or CORD, even in patients with the same genotype, excluding possible genotype-phenotype correlations.[15,17,25] It is of note, that detailed review of our cohort has demonstrated that overlapping features of both categories were present concurrently in a large proportion of patients; with early drop in acuity and central visual field loss in patients with 'RCD', and nyctalopia and peripheral visual field loss as presenting symptoms in individuals with 'CORD' (Supplementary Table 4).[15,17,25] It appears that unlike the majority of other genetic causes of IRD, the boundaries between the two categories are not as clear, with many patients presenting with both cone and rod-related symptoms simultaneously (36% per imaging, 34% per ERG, and 34 % per initial symptoms).

This has been noted in previous reports of smaller cohorts, but is extended and confirmed in our larger, genetically and ethnically diverse cohort (Supplementary Table 2).[5,17]

The rate of VA decline was high compared to other genotypes (*CRB1*-RP 0.07 LogMAR/year and *RPGR*(ORF15) 0.02/year),[24,26] and even faster in the 25-40 year old group, suggesting preserved acuity until the third decade of life, followed by a more rapid decline. Yet, VA encompassed an incredibly broad range both at baseline and during follow-up, with over 50% of individuals above 40 years old still having no or mild visual impairment as per the WHO classification; indicating the variable prognosis associated with *CERKL*-retinal dystrophy. Asymmetric BCVA was seen in 21% of patients at baseline, which is high compared to other conditions including Stargardt disease (reported at 8%).[27] If a less stringent measure of VA asymmetry was applied, a yet greater asymmetry would be noted.

Macular hyperautofluorescent punctate lesions visible with BAF were found to correspond with subretinal hyperreflective material on OCT (Figure 4A & B). This feature was also highlighted by Sengillo *et al.*,[28] who described them as becoming denser as the disease progressed. In our cohort, we observed two scenarios over time; one in which the hyperautofluorescent lesions were replaced by hypoautofluorescence and increased atrophy, and another where indeed these dots increased in number as the atrophy grew (Figure 4C & D). The fact that these lesions are excited by 488 nm blue light could indicate that they are at least partly composed by lipofuscin/lipofuscin-like and N-retinylidene-N-retinylethanolamine (A2E)/A2E-related material, suggesting that they may correspond to photoreceptor debris resultant from *CERKL*-mediated decreased RPE phagocytosis.[29,30] Similar dots/subretinal debris-material has been reported in *MERTK*-retinopathy,[31] a dysfunctional phagocytosis-associated dystrophy.

A novel, less-common finding in our cohort is the presence of a large hyperautofluorescent ring extending beyond the posterior pole and encompassing the optic disc (5 patients, Supplementary Table 2 & Figure 3A). This pattern has also been seen in other IRDs including dominant *NR2E3*- and *EYS*-related retinopathies, representing in both cases the boundaries between affected and unaffected retina.[32,33] Yet, in *NR2E3*, this ring grew centrifugally towards the mid-periphery and in *EYS* it shrunk over time. In our case, the ring grew and became less well-defined in the majority of the patients, in keeping with *NR2E3*-IRD. Other features to consider in *CERKL*-retinopathy are peripapillary atrophy which, although not pathognomonic of *CERKL*, may be

useful when distinguishing between this gene and *ABCA4* (classically associated with peripapillary sparing);[34] and ERM with inner retinal wrinkling. The latter was reported in up to 22.8% of patients with RP; however, in our cohort it was seen in nearly three times that proportion, and in previous series it affected 2 and 3 out of 6 patients.[15,35,36]

The electrophysiological profiles in our series were diverse, with 16/30 having a similar degree of rod and cone photoreceptor dysfunction and most others (8/30) having a rod-cone pattern of dysfunction. A minority had CORD and MD (3/30 each), in keeping with previous reports of ERG variability.[5,10,15] There was overlap in ERG phenotypes associated with DN and NDN genotypes, but a large majority of nullizygous cases had severe generalized photoreceptor dysfunction, including the youngest individuals. Those with NDN variants included two older patients with MD (normal ERG) and most of those with relatively mild retinal dysfunction. An apparent disconnect between ERG and initial symptoms was seen in 4 patients with RCD per electrophysiology and initial symptoms of opposite phenotypes (CORD and MD; ID 6A, 10C, 23, & 24), all with equal central and peripheral involvement in imaging. Although in some of these cases the symptoms may evolve to eventually match the ERG phenotype (ERG functioning as a predictor, as in *ABCA4*-Stargardt disease),[37] in others the ERG may represent an additional piece of information that characterizes the patients disease, not necessarily matching the remaining assessments. The lack of clear correlation between the ERG findings, symptoms, and retinal imaging (Supplementary Table 2), highlights the need for comprehensive phenotypic assessment.

In our study, p.(Arg283Ter) was the most common variant, in concordance with other reports.[17] The second most common change, p.(Arg106Ser), was described to possibly lead to cellular death given its highly conserved location within the protein, functioning as a null allele despite being missense.[38] We have demonstrated a degree of genotype-phenotype correlation, with patients harboring DN genotypes displaying signs of increased severity when compared to those with NDN, including younger age of onset, greater visual impairment, more retinal pigmentary disturbance with often concomitant peripheral and macular circumscribed atrophic lesions, and more profound ERG dysfunction. However, we also noted overlap between the 2 genotypic groups and the aforementioned signs of disease severity - in keeping with the previously well-

documented heterogeneity of IRDs. Investigation of further *CERKL* cases will help to extend our observations.

Over 20 different *CERKL* transcripts have been found in the human retina, due to extensive alternative splicing and multiple translational start sites, with preferential isoform expression in different cells.[39,40] A double knockout zebrafish model found that rods degenerated earlier and more significantly than cones,[30] yet a knockdown-knockout mouse model found cones to be more affected.[40] The models agreed on photoreceptor outer segment abnormalities, accumulating in the interphotoreceptor matrix and becoming very long and disorganized, suggestive of decreased RPE phagocytosis.[30,40] *CERKL* has recently been characterized as an oxidative stress protective gene within RPE cells, hence decreased RPE function may occur in its abscence.[14] It is possible that different disease-causing variants have greater impact on certain transcripts preferentially expressed in cones versus rods, or equally in both, resulting in the different phenotypes and symptoms observed in our study. Furthermore, certain variants could affect how CERKL interacts with other proteins, interfering with its complex function and regulation, potentially again with different impacts on rods versus cones. Environmental or other genetic modifying factors may also play a role in the variable phenotypic presentations. Future functional studies may shed further light on this topic.

Given the link between *CERKL* and oxidative stress, antioxidant therapeutic approaches might have a positive effect on this condition.[41] These are currently under investigation for other IRD genes such as *ABCA4*, and if successful might also prove useful for *CERKL* retinopathy.[42,43] Similarly, slowing down the visual cycle could decrease the generation of A2E and limit the formation of macular hyperautofluorescent punctate lesions. RBP4-inhibitors could be helpful if proven beneficial in *ABCA4* Stargardt disease (NCT05244304). *CERKL* would also be a good candidate for gene therapy, given its reasonable window of opportunity. However, due to its size not fitting in a regular AAV-vector, it would require alternative vectors or dual vector technology.

Our study limitations include its retrospective nature, the different proportion of individuals in the DN and NDN subgroups, not all data being available for every individual, and data being acquired with various methods and protocols. The lack of visual field data reflects the real-world environment in which clinical data were collected. These are to a large extent offset by the large

number of genetically-confirmed patients, their wide age-range and ethnic background, and the international nature of the cohort.

This study represents the largest series of patients with *CERKL*-associated retinopathy to date. We characterised detailed clinical features, disease progression, estimating the rate of visual acuity change and providing insights into genotype-phenotype correlations. *CERKL*-retinopathy has a broad phenotypic spectrum ranging from isolated macular dystrophy to severe generalised retinal involvement. retinal-wide disease and it often does not follow the classical RCD/CORD dichotomy. and it can present with both cone- and rod-related symptoms at the outset, associated with structural and functional signs of both cone and rod dysfunction/loss. In many patients, a greater rate of central vision loss may occur in the third decade. Common retinal changes observed in *CERKL*-retinopathy include peripheral and macular circular areas of chorioretinal atrophy, little to no pigment dispersion, and fine hyperautofluorescent macular dots. The nature of retinal dysfunction often cannot be inferred reliably from clinical signs or imaging alone, highlighting the importance of comprehensive phenotyping.

References

1. Georgiou M, Fujinami K, Michaelides M. Inherited retinal diseases: Therapeutics, clinical trials and end-points - A review. *Clin Experiment Ophthalmol*. Published online March 2021. doi:10.1111/ceo.13917

2. Liew G, Michaelides M, Bunce C. A comparison of the causes of blindness certifications in England and Wales in working age adults (16-64 years), 1999-2000 with 2009-2010. *BMJ Open*. 2014;4(2):e004015. doi:10.1136/bmjopen-2013-004015

3. Pontikos N, Arno G, Jurkute N, et al. Genetic Basis of Inherited Retinal Disease in a Molecularly Characterized Cohort of More Than 3000 Families from the United Kingdom. *Ophthalmology*. 2020;127(10):1384-1394. doi:10.1016/j.ophtha.2020.04.008

4. Birtel J, Eisenberger T, Gliem M, et al. Clinical and genetic characteristics of 251 consecutive patients with macular and cone/cone-rod dystrophy. *Sci Rep*. 2018;8(1):4824. doi:10.1038/s41598-018-22096-0

5. Auslender N, Sharon D, Abbasi AH, Garzozi HJ, Banin E, Ben-Yosef T. A Common Founder Mutation of CERKL Underlies Autosomal Recessive Retinal Degeneration with Early Macular Involvement among Yemenite Jews. *Invest Ophthalmol Vis Sci*. 2007;48(12):5431-5438. doi:10.1167/iovs.07-0736

6. Zahid S, Branham K, Schlegel D, et al. *Retinal Dystrophy Gene Atlas*. Springer; 2018.

7. Habibi I, Falfoul Y, Turki A, et al. Genetic spectrum of retinal dystrophies in Tunisia. *Sci Rep*. 2020;10(1):11199. doi:10.1038/s41598-020-67792-y

8. Martin-Merida I, Avila-Fernandez A, Del Pozo-Valero M, et al. Genomic Landscape of Sporadic Retinitis Pigmentosa: Findings from 877 Spanish Cases. *Ophthalmology*. 2019;126(8):1181-1188. doi:https://doi.org/10.1016/j.ophtha.2019.03.018

9. Tuson M, Marfany G, Gonzàlez-Duarte R. Mutation of CERKL, a novel human ceramide kinase gene, causes autosomal recessive retinitis pigmentosa (RP26). *Am J Hum Genet*. 2004;74(1):128-138. doi:10.1086/381055

10. Avela K, Sankila EM, Seitsonen S, et al. A founder mutation in CERKL is a major cause

of retinal dystrophy in Finland. *Acta Ophthalmol*. 2018;96(2):183-191. doi:10.1111/aos.13551

11. Roberts L, Ratnapriya R, du Plessis M, Chaitankar V, Ramesar RS, Swaroop A. Molecular Diagnosis of Inherited Retinal Diseases in Indigenous African Populations by Whole-Exome Sequencing. *Invest Ophthalmol Vis Sci*. 2016;57(14):6374-6381. doi:10.1167/iovs.16-19785

12. Riera M, Burguera D, Garcia-Fernàndez J, Gonzàlez-Duarte R. CERKL knockdown causes retinal degeneration in zebrafish. *PLoS One*. 2013;8(5):e64048. doi:10.1371/journal.pone.0064048

13. Meyer JM, Lee E, Celli A, et al. CERKL is upregulated in cutaneous squamous cell carcinoma and maintains cellular sphingolipids and resistance to oxidative stress*. *Br J Dermatol*. 2021;185(1):147-152. doi:https://doi.org/10.1111/bjd.19753

14. García-Arroyo R, Gavaldà-Navarro A, Villarroya F, Marfany G, Mirra S. Overexpression of CERKL Protects Retinal Pigment Epithelium Mitochondria from Oxidative Stress Effects. *Antioxidants (Basel, Switzerland)*. 2021;10(12). doi:10.3390/antiox10122018

15. Aleman TS, Soumittra N, Cideciyan A V, et al. CERKL mutations cause an autosomal recessive cone-rod dystrophy with inner retinopathy. *Invest Ophthalmol Vis Sci*. 2009;50(12):5944-5954. doi:10.1167/iovs.09-3982

16. Littink KW, Koenekoop RK, van den Born LI, et al. Homozygosity mapping in patients with cone-rod dystrophy: novel mutations and clinical characterizations. *Invest Ophthalmol Vis Sci*. 2010;51(11):5943-5951. doi:10.1167/iovs.10-5797

17. Avila-Fernandez A, Riveiro-Alvarez R, Vallespin E, et al. CERKL Mutations and Associated Phenotypes in Seven Spanish Families with Autosomal Recessive Retinitis Pigmentosa. *Invest Ophthalmol Vis Sci*. 2008;49(6):2709-2713. doi:10.1167/iovs.07-0865

18. Day AC, Donachie PHJ, Sparrow JM, Johnston RL. The Royal College of Ophthalmologists' National Ophthalmology Database study of cataract surgery: report 1, visual outcomes and complications. *Eye (Lond)*. 2015;29(4):552-560. doi:10.1038/eye.2015.3

19. Invernizzi A, Pellegrini M, Acquistapace A, et al. Normative Data for Retinal-Layer Thickness Maps Generated by Spectral-Domain OCT in a White Population. *Ophthalmol Retin*. 2018;2(8):808-815.e1. doi:https://doi.org/10.1016/j.oret.2017.12.012

20. Tatour Y, Ben-Yosef T. Syndromic Inherited Retinal Diseases: Genetic, Clinical and Diagnostic Aspects. *Diagnostics*. 2020;10(10). doi:10.3390/diagnostics10100779

21. Robson AG, Frishman LJ, Grigg J, et al. ISCEV Standard for full-field clinical electroretinography (2022 update). *Doc Ophthalmol*. 2022;144(3):165-177. doi:10.1007/s10633-022-09872-0

22. Georgiou M, Fujinami K, Vincent A, et al. KCNV2-Associated Retinopathy: Detailed Retinal Phenotype and Structural Endpoints-KCNV2 Study Group Report 2. *Am J Ophthalmol*. 2021;230:1-11. doi:10.1016/j.ajo.2021.03.004

23. Richards S, Aziz N, Bale S, et al. Standards and guidelines for the interpretation of sequence variants: a joint consensus recommendation of the American College of Medical Genetics and Genomics and the Association for Molecular Pathology. *Genet Med*. 2015;17(5):405-424. doi:10.1038/gim.2015.30

24. Daich Varela M, Georgiou M, Alswaiti Y, et al. CRB1-Associated Retinal Dystrophies: Genetics, Clinical Characteristics, and Natural History. *Am J Ophthalmol*. 2023;246:107-121. doi:https://doi.org/10.1016/j.ajo.2022.09.002

25. Rodríguez-Muñoz A, Aller E, Jaijo T, et al. Expanding the Clinical and Molecular Heterogeneity of Nonsyndromic Inherited Retinal Dystrophies. *J Mol Diagn*. 2020;22(4):532-543. doi:10.1016/j.jmoldx.2020.01.003

26. Talib M, van Schooneveld MJ, van Duuren RJG, et al. Long-Term Follow-Up of Retinal Degenerations Associated With LRAT Mutations and Their Comparability to Phenotypes Associated With RPE65 Mutations. *Transl Vis Sci Technol*. 2019;8(4):24. doi:10.1167/tvst.8.4.24

27. Fakin A, Robson AG, Fujinami K, et al. Phenotype and Progression of Retinal Degeneration Associated With Nullizigosity of ABCA4. *Invest Ophthalmol Vis Sci*. 2016;57(11):4668-4678. doi:10.1167/iovs.16-19829

28. Sengillo JD, Cho GY, Paavo M, et al. Hyperautofluorescent Dots are Characteristic in Ceramide Kinase Like-associated Retinal Degeneration. *Sci Rep*. 2019;9(1):876. doi:10.1038/s41598-018-37578-4

29. Daich Varela M, Esener B, Hashem S, Guimaraes T, Georgiou M, Michaelides M. Structural evaluation in inherited retinal diseases. *Br J Ophthalmol*. Published online 2021.

30. Yu S, Li C, Biswas L, et al. CERKL gene knockout disturbs photoreceptor outer segment phagocytosis and causes rod-cone dystrophy in zebrafish. *Hum Mol Genet*. 2017;26(12):2335-2345. doi:10.1093/hmg/ddx137

31. Audo I, Mohand-Said S, Boulanger-Scemama E, et al. MERTK mutation update in inherited retinal diseases. *Hum Mutat*. 2018;39(7):887-913. doi:https://doi.org/10.1002/humu.23431

32. Sengillo JD, Lee W, Nagasaki T, et al. A Distinct Phenotype of Eyes Shut Homolog (EYS)-Retinitis Pigmentosa Is Associated With Variants Near the C-Terminus. *Am J Ophthalmol*. 2018;190:99-112. doi:https://doi.org/10.1016/j.ajo.2018.03.008

33. Murro V, Mucciolo DP, Sodi A, et al. Novel clinical findings in autosomal recessive NR2E3-related retinal dystrophy. *Graefe's Arch Clin Exp Ophthalmol*. 2019;257(1):9-22. doi:10.1007/s00417-018-4161-z

34. Khan KN, Kasilian M, Mahroo OAR, et al. Early Patterns of Macular Degeneration in ABCA4-Associated Retinopathy. *Ophthalmology*. 2018;125(5):735-746. doi:10.1016/j.ophtha.2017.11.020

35. Liew G, Strong S, Bradley P, et al. Prevalence of cystoid macular oedema, epiretinal membrane and cataract in retinitis pigmentosa. *Br J Ophthalmol*. 2019;103(8):1163-1166. doi:10.1136/bjophthalmol-2018-311964

36. Sen P, Maitra P, Natarajan S, et al. CERKL mutation causing retinitis pigmentosa(RP) in Indian population - a genotype and phenotype correlation study. *Ophthalmic Genet*. 2020;41(6):570-578. doi:10.1080/13816810.2020.1814347

37. Fujinami K, Lois N, Davidson AE, et al. A longitudinal study of stargardt disease: clinical

and electrophysiologic assessment, progression, and genotype correlations. *Am J Ophthalmol*. 2013;155(6):1075-1088.e13. doi:10.1016/j.ajo.2013.01.018

38. Ali M, Ramprasad VL, Soumittra N, et al. A missense mutation in the nuclear localization signal sequence of CERKL (p.R106S) causes autosomal recessive retinal degeneration. *Mol Vis*. 2008;14:1960-1964.

39. Garanto A, Riera M, Pomares E, et al. High transcriptional complexity of the retinitis pigmentosa CERKL gene in human and mouse. *Invest Ophthalmol Vis Sci*. 2011;52(8):5202-5214. doi:10.1167/iovs.10-7101

40. Domènech EB, Andrés R, López-Iniesta MJ, et al. A New Cerkl Mouse Model Generated by CRISPR-Cas9 Shows Progressive Retinal Degeneration and Altered Morphological and Electrophysiological Phenotype. *Invest Ophthalmol Vis Sci*. 2020;61(8):14. doi:10.1167/iovs.61.8.14

41. B Domènech E, Marfany G. The Relevance of Oxidative Stress in the Pathogenesis and Therapy of Retinal Dystrophies. *Antioxidants (Basel, Switzerland)*. 2020;9(4). doi:10.3390/antiox9040347

42. Piotter E, McClements ME, MacLaren RE. Therapy Approaches for Stargardt Disease. *Biomolecules*. 2021;11(8). doi:10.3390/biom11081179

43. Daich Varela M, Michaelides M. RDH12 retinopathy: clinical features, biology, genetics and future directions. *Ophthalmic Genet*. Published online May 2022:1-6. doi:10.1080/13816810.2022.2062392

Figure legends

Figure 1: Visual acuity in *CERKL*-associated retinal dystrophy. A) Mean visual acuity + standard deviation (SD) in patients from our cohort at their baseline visit, divided into 3 age groups. B) WHO visual impairment categories in the same age groups at their baseline visit. C) Linear regression showing a significant association between age and best corrected visual acuity at baseline visit, for both OD ($p = 0.0002$) and OS ($p < 0.0001$).

Figure 2: Fundus features of patients with *CERKL*-associated retinal dystrophy. A) 39-year-old patient with both macular and peripheral circumscribed patches of chorioretinal atrophy (CRA) and moderate pigment deposits. The patient had a rod-cone dystrophy on electrophysiological testing (ERG, ID 10) and reported decreased central vision as her initial symptom, at age 15. B) 21-year-old showing only macular atrophy, a hyperautofluorescent ring at the posterior pole, and no pigmentary changes. He had a cone-rod dystrophy on ERG (ID 27) and described decreased central vision and light sensitivity since age 17. C) Retinal images from a 45-year-old patient with predominantly peripheral involvement, with CRA patches in the periphery and mid-periphery and diffuse pigment dispersion. She did not have an ERG assessment and mentioned concurrent decreased central vision and nyctalopia since age 36.

Figure 3. Less common retinal features found in our *CERKL*-associated retinal dystrophy cohort. A) Autofluorescence (AF) imaging from a 30-year-old man, with a hyperautofluorescent ring at the posterior pole, extending beyond the temporal vascular arcades and encompassing the optic disc. Macular OCT scan showing remnant subfoveal ellipsoid zone (EZ) line. The patient had equally affected rod and cone ERG responses (ID 22) and was diagnosed with a 'macular dystrophy' at age 19. B) 32-year-old patient with a hypoautofluorescent pattern that follows the vascular arcades. Macular OCT scan is positive for outer retinal degeneration and an epiretinal membrane (ERM). She had equal rod and cone dysfunction on ERG (ID 3) and reported decreased central vision as her initial symptom, at age 7. C) AF imaging from a 15-year-old patient uneven autofluorescence and hypoautofluorescent dots inferiorly. Macular OCT shows minimal subfoveal EZ and outer retinal degeneration. He had equal rod and cone impairment on ERG (ID 13) and developed decreased central vision at age 13. D) 55-year-old patient with a few peripheral CRA patches and an abnormal autofluorescence pattern, with a preserved nasal, mid-peripheral area. Macular OCT shows minimal subfoveal EZ, outer retinal degeneration and

ERM. She had a rod-cone dystrophy pattern on ERG (ID 24) and described decreased central vision since age 23. E) 9-year-old (ID 41, brother of ID 13 -displayed on C-). There is vessel thinning, mild retinal mottling and uneven autofluorescence. Bilateral macular OCT is positive for outer retinal loss, with preserved central EZ and overall architecture. He remains asymptomatic (last visit at age 11).

Figure 4. Macular optical coherence tomography (OCT) and Heidelberg imaging. A) Correlation of blue fundus autofluorescence (BAF), infrared (IR) and OCT imaging of patient ID 14 at 20 years of age, with rod-cone dystrophy on ERG and mixed rod and cone symptoms at onset. A hyperautofluorescent dot is seen in BAF next to the vessel (green square), hyporeflective in IR and subretinal hyperreflective material evident in that location on OCT. B) Correlation of BAF, IR and OCT imaging of patient ID 20 at age 27. Here is another example of a hyperautofluorescent dot on BAF, hyporeflective on IR and subretinal hyperreflective material in that location. C) Fundus autofluorescence images of a patient clinically diagnosed with *CERKL*-associated retinitis pigmentosa (ID 43). To the left is the patient at 26 years of age and to the right that same patient at age 37. Scattered atrophy is seen in the posterior pole and mid-periphery, with hyperautofluorescent fine dots surrounding the posterior pole at an early stage, and few dots remaining in the most recent image, these having been largely replaced by hypoautofluorescence. Macular OCT scans show a narrowed EZ line and loss of retinal layering over follow up. D) Fundus autofluorescence changes in patient ID 20, with an electrophysiological diagnosis of cone-rod dystrophy and mixed rod and cone symptoms at onset. To the left is the posterior pole at age 18 and to the right at age 33. In this case, the central atrophy enlarged, and the hyperautofluorescent dots increased in number/ became more noticeable over time. Longitudinal macular OCT shows more profound outer retinal atrophy and poor retinal architecture over time.

Figure 5. Full field ERG and PERG findings summarized in 30 patients tested according the ISCEV standard; a) The amplitudes of the DA 10 ERG a-wave, LA 30 Hz ERG, LA 3 ERG b-wave and PERG P50 component are plotted against the primary axis as a percentage of the age-matched lower limit of the reference range (horizontal broken line), with values arranged in ascending order of DA 10 ERG a-wave amplitude for clarity. The LA 30 Hz peak times are plotted against the secondary axis as a difference from the age-matched upper limit of the

reference range (horizontal dotted line). b) The age of the patients at the time of testing, arranged in same order as in a). Patients with NDN variants include those numbered 11, 14, 20, 22, 23, 25, 27, 29 and 30 (highlighted with vertical arrows). All DA and LA ERGs and PERGs were undetectable in patients 1-5, 6 and 7.

Figure 6. Representative full-field and pattern ERGs from three patients and one control subject for comparison; a) patient 2 (aged 30 years); b) patient 22 (29 years); c) patient 30 (47 years); d) representative control ("normal") recordings. Numbering of patients corresponds to that used in Figure 5. Data are shown for the right eyes only, as all recordings showed a high degree of inter-ocular symmetry. Patient traces are superimposed to demonstrate reproducibility. Broken lines replace blink artefacts for clarity. The full-field ERGs in patients 2 and 22 are consistent with a rod and cone photoreceptor dystrophy affecting rods and cones similarly, with PERG evidence of macular involvement, more severe in patient 2. The ERGs in patient 21 are in keeping with a rod-cone dystrophy, with a detectable but subnormal PERG, indicating macular involvement. The undetectable PERG in case 30 is consistent with severe macular dysfunction with no full-field ERG evidence of generalized retinal dysfunction.

Figure 8. Graphic representation of the *CERKL* gene and protein, with details on functional domains. *CERKL* (Transcript; NM_001030311.2, ENST00000339098.9, Uniprot accessions: Q49MI3) contains 13 exons that encode a 532 amino acid protein containing a disordered region, nuclear localization signal 1 motif, nuclear localization signal 2 motif, and a diacylglycerol kinase catalytic domain. Seven nonsense, 6 missense, and 2 small deletion/frameshift variants detected in this cohort are demonstrated. Novel variants are highlighted by a *.

Table 1. Clinical Characteristics of Patients with *CERKL*-Associated Retinal Dystrophy

Characteristics	Patients (n=47)
Families	37
Gender (n (%))	
· Female	22 (47)
· Male	25 (53)
Age at first examination (mean ± SD, years)	29.6 ± 13.9
Age at last examination (mean ± SD, years)	39.2 ± 16.6
Follow-up time (mean ± SD, years)	9.1 ± 7.4
Ethnicity (n (%))	34 (72)
· Asian	19 (56)
· White European	13 (38)
· African descent	2 (6)
Age of onset (mean ± SD, years)	19.8 ± 9 years
Reported first symptom (n (%))	
· Central vision loss	19 (40)
· Concurrent central vision loss and nyctalopia	16 (34)
· Night blindness	5 (11)
· Others (scotomas, photophobia, colour vision issues)	7 (15)
Spherical equivalent refractive error (mean ± SD, D)	-1.9 ± 2.8
Funduscopic examination (n (%))	
· Circumscribed areas of atrophy in the macula	27 (57)
· Fine white dots at the macula and perimacula	23 (49)
· Peripheral punched-out-like areas of chorioretinal atrophy	21 (45)
· Hyperautofluorescent ring at the posterior pole (Robson ring)	11 (23)
· Ring including the optic disc	5 (11)
· Hypoautofluorescent nummular dots that followed the vascular arcades	5 (11)
· Mottled/uneven retinal aspect	3 (6)
· foveal-sparing maculopathy	3 (6)
· Abnormal autofluorescence pattern	4 (9)
Retinal pigment deposits (n (%))	42 (89)
· None	18 (38)
· Minimal	15 (32)
· Moderate	3 (6)
· Dense, diffuse	6 (13)
Most affected retinal area by UWF imaging (n (%))	39 (82)
· Macula	11 (23)
· Periphery	11 (23)
· Similar both	17 (36)
Full-field electroretinography (n (%))	30 (64)
· Similar cone and rod involvement	16 (53)
· Rod-cone pattern	8 (27)
· Cone-rod pattern	3 (10)
· Macular dystrophy (normal full-field ERG)	3 (10)

Abbreviations: SD: standard deviation; n: number; D: diopters; UWF: ultrawide-field; ERG: electroretinogram

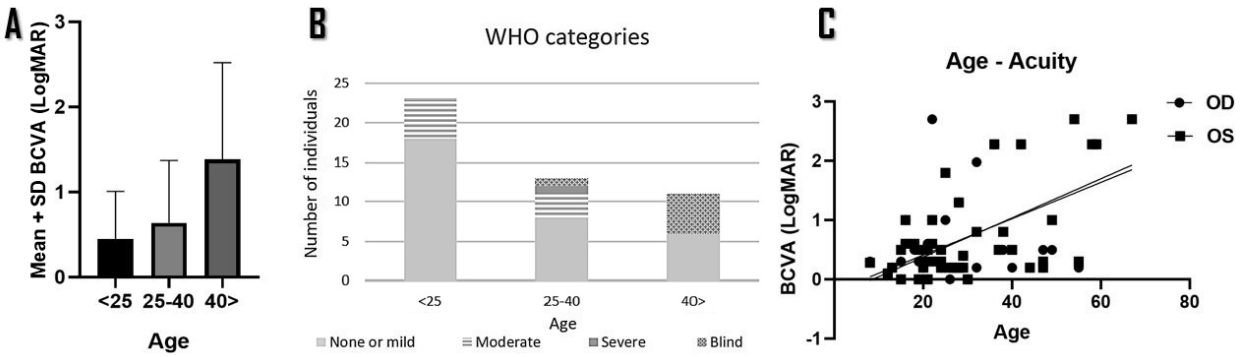

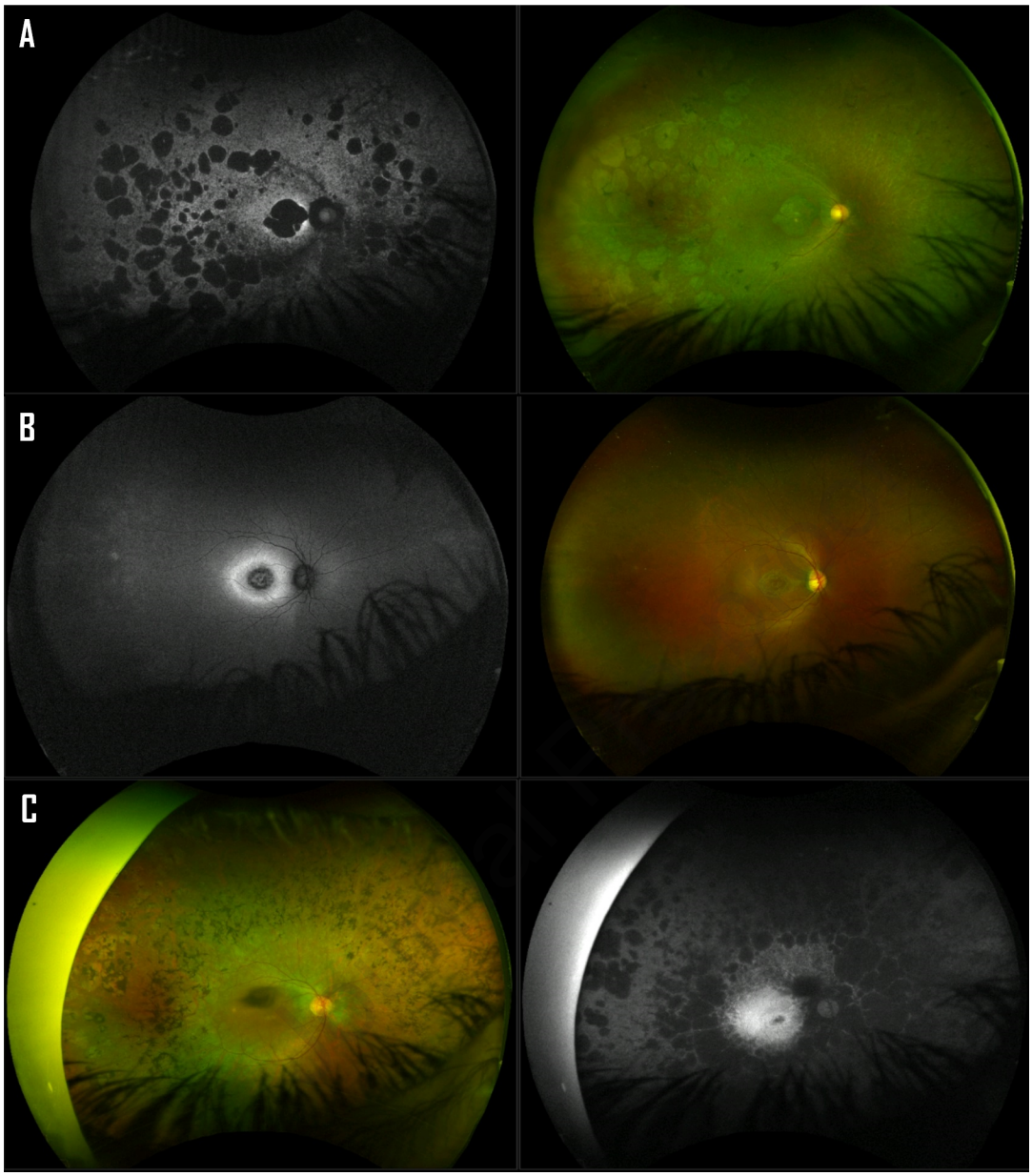
A
B
C

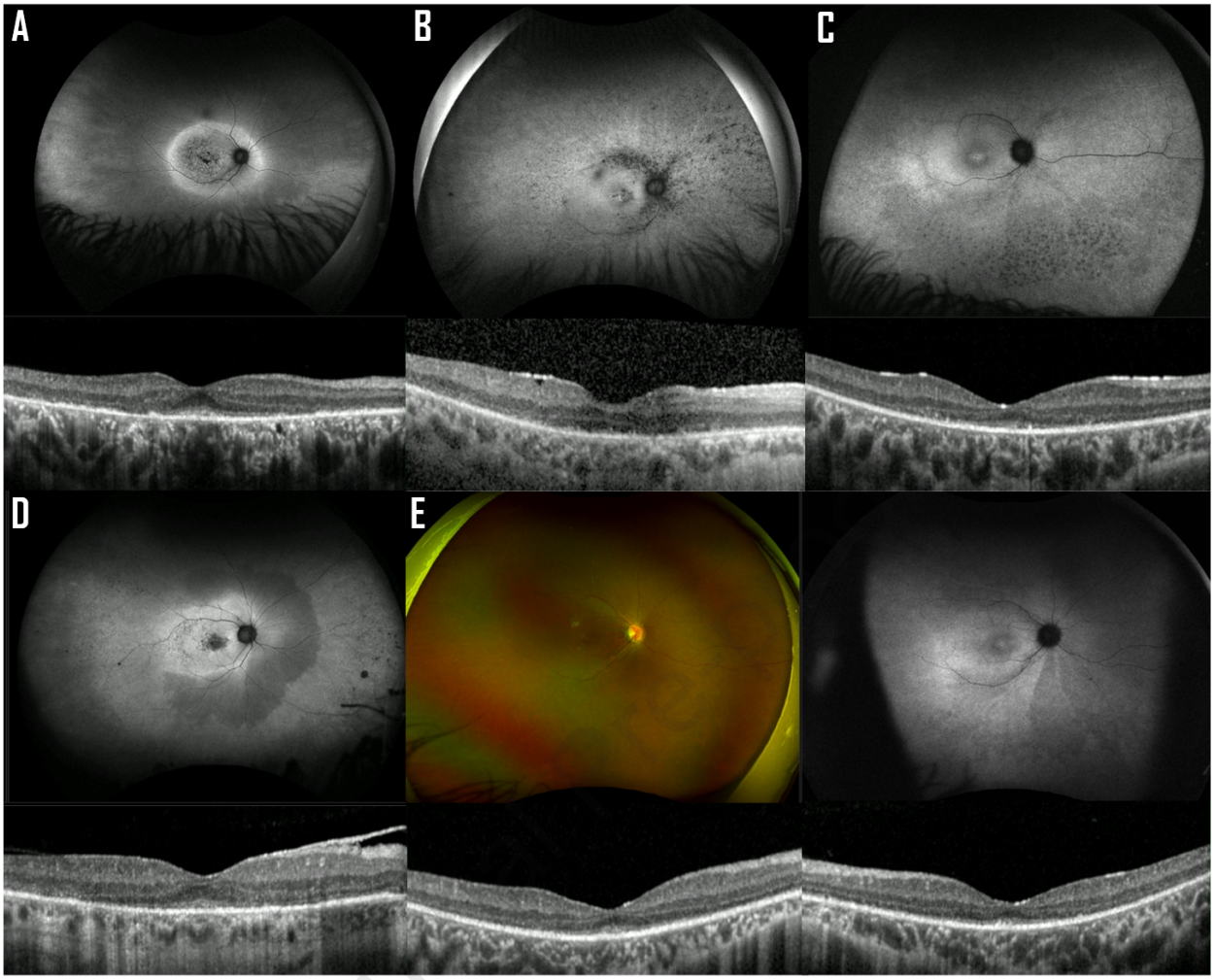

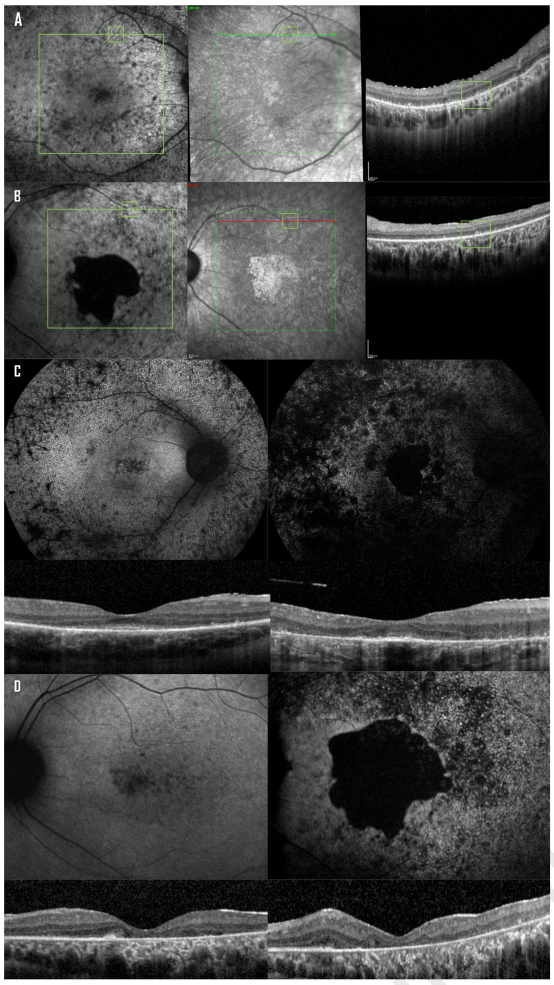

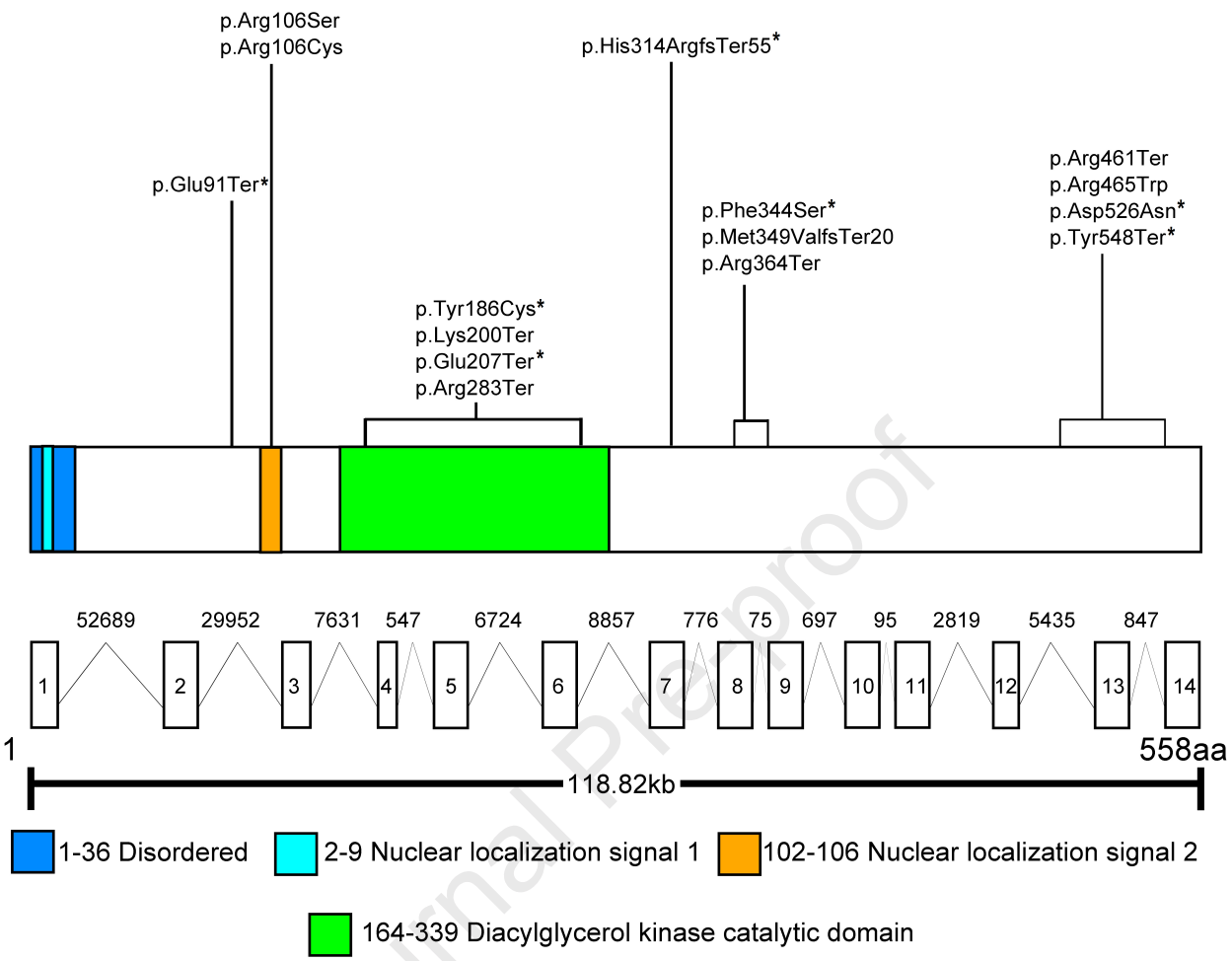

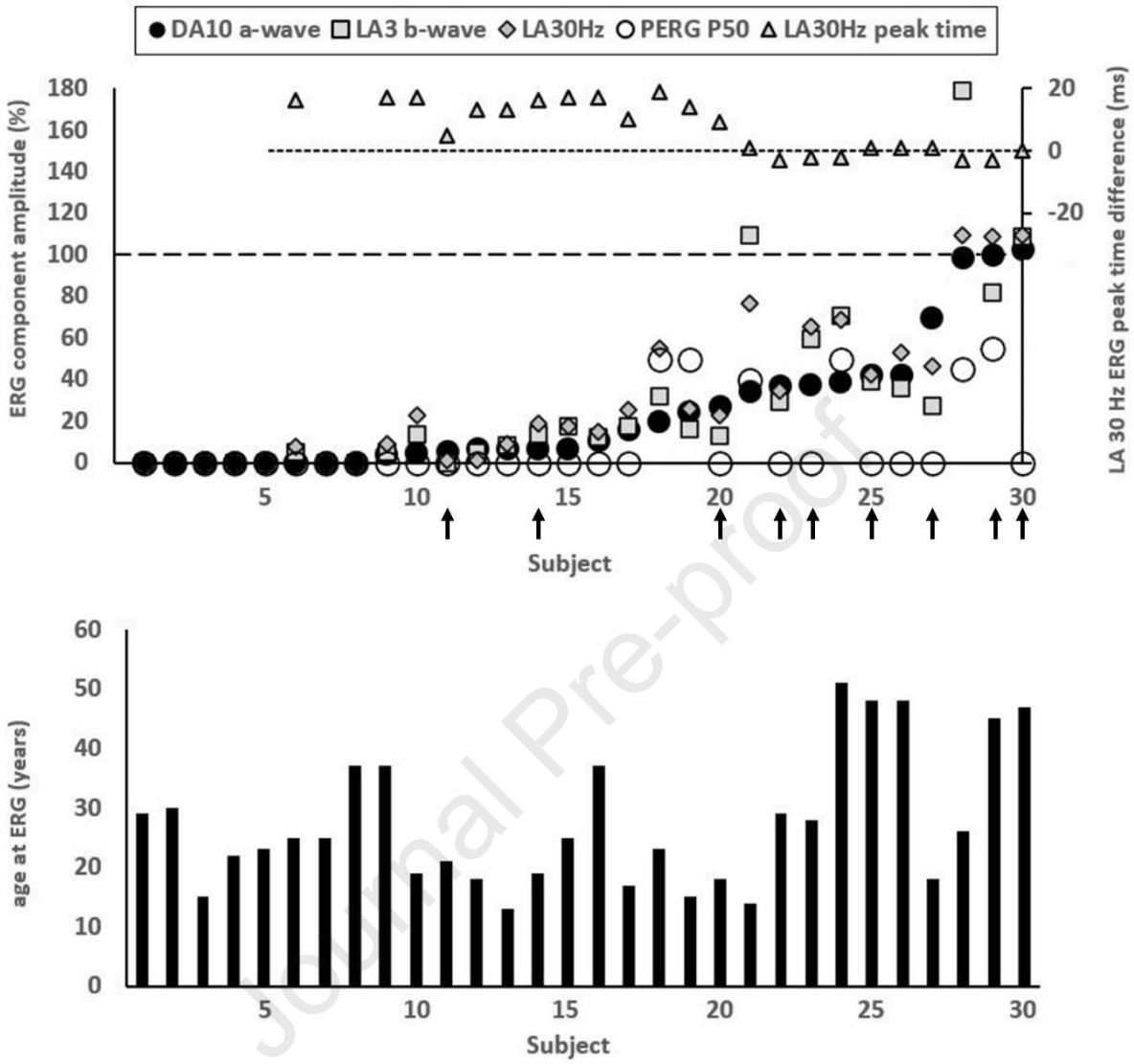

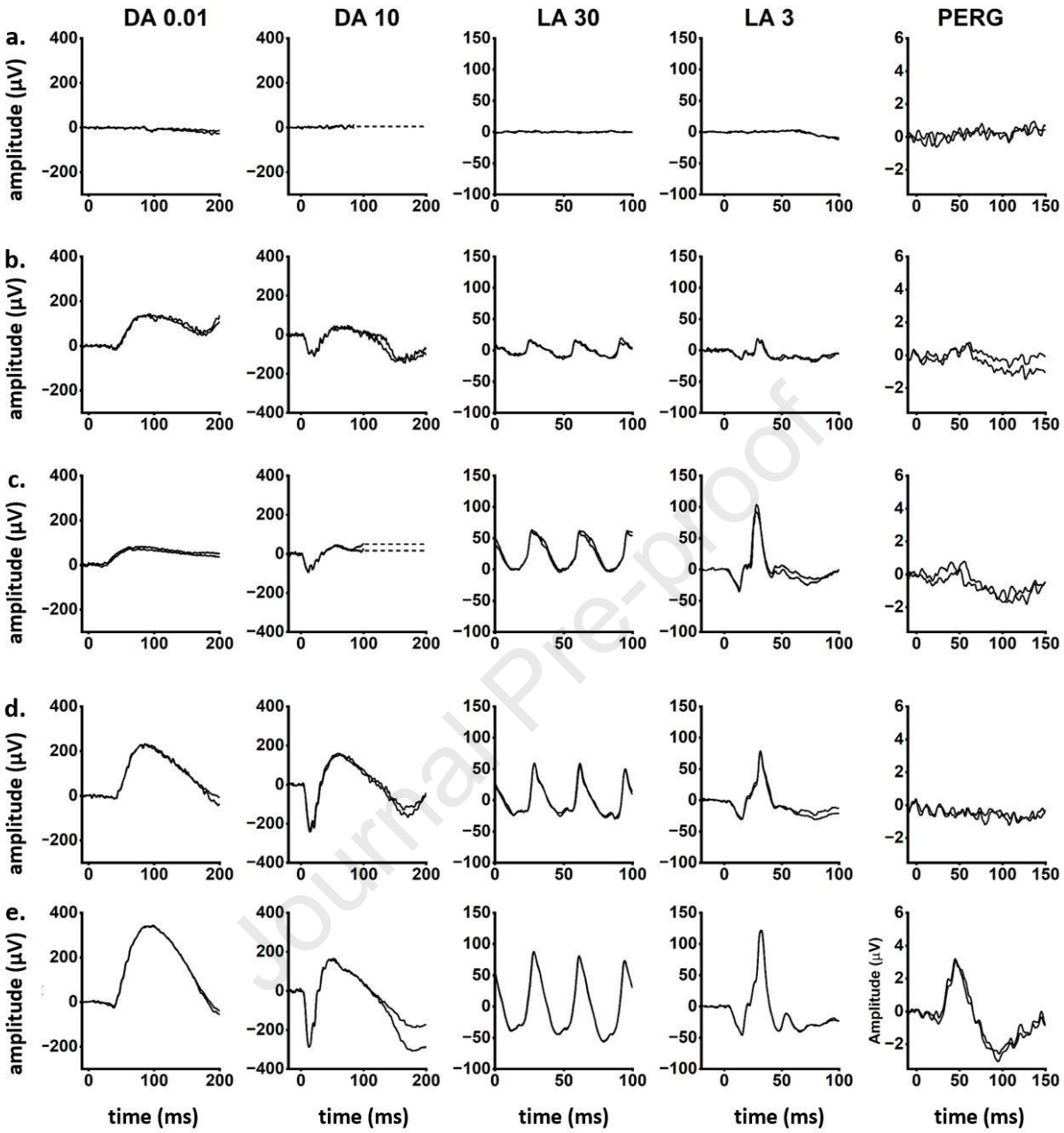

CERKL-retinopathy encompasses isolated macular disease to severe retina-wide involvement, with a range of functional phenotypes, generally not fitting in the rod-cone/cone-rod dichotomy. Nullizygous cases are often more severe.